

## Design of an Optical Thermal Sensor Based on Polydimethylsiloxane Polymers

Urooj aftab khilji <sup>1</sup>, Yousuf Khan<sup>2</sup>

<sup>1</sup> Department of Electronic Engineering, Balochistan University of Information Technology, Engineering and Management Sciences, Quetta 87300, Pakistan

<sup>2</sup> Nanophotonics Research Group, Department of Electronic Engineering, Balochistan University of Information Technology, Engineering and Management Sciences, Quetta 87300, Pakistan

**DOI:** <https://doi.org/10.63163/jpehss.v4i1.1149>

### Abstract

The study employed polydimethylsiloxane polymers with the purpose of developing an optical temperature sensor. It will have practical uses in biosensing and temperature-sensing. The PDMS polymer will be applied onto the photonic crystal hole and subsequently filled with it. When the voids in the polymer are filled, a functional layer will form on the surface of the photonic crystal, despite the polymer's inherent liquid state and flexibility. In order to test bio-sensing capabilities, we subjected polymers to a controlled temperature variation environment, which resulted in a change in the reflective index as a result of temperature. Low temperatures result in a high reflecting index, whereas high temperatures lead to a low reflective index, causing transparency owing to light. The unit cell design will be subjected to experimental modifications to enhance the accuracy of the results, utilizing Meep Python, a simulation program

**Keywords:** optical thermal sensor; PDMS-based sensing; dielectric photonic crystals

### Introduction

Optical thermal sensors have garnered significant attention due to their numerous advantages, including immunity to electromagnetic interference, rapid response times, heightened sensitivity, non-intrusive detection, and the capability to measure temperature distribution in their immediate vicinity, among other benefits. Optical thermal sensing refers to a method that categorizes temperatures by analyzing the luminescence, fluorescence lifetime, or other luminous characteristics of optical materials. The utilization of temperature sensors has experienced an increase [ 5] . Optical temperature sensors are a specialized type of sensor that utilizes optical technology, typically fiber optics, to measure temperature. Recently, several researches have suggested the use of optical fiber for refractive file detection. Plasmonic sensors, detection recording, exceptional safeguards, Fano-reverberation enabled sensors, fiber-optic-based detection, and nanocavity-based detection are all techniques that have been considered for optical temperature sensing. Additionally, studies have demonstrated that thermally responsive substances, such as ethanol and PDMS, can be utilized alongside plasmonic waveguides for the purpose of detecting heat. [1]

Three-dimensional photonic crystals (PhCs) have been extensively studied for various sensing applications, such as temperature monitoring, biological sensing, bacteria detecting, fluid sensing, gas sensing, and refractive index sensing in general[6]. Recently, Optical-fiber-based refractive index sensing has been proposed in numerous research studies [2]. Plasmonic waveguides have

been utilized in conjunction with thermally sensitive substances like ethanol and PDMS to showcase thermal sensing capabilities. PDMS is renowned for its outstanding rheological characteristics, commonly referred to as flow properties. PDMS exhibits a transparent appearance and is inherently non-toxic, innocuous, and non-combustible. PDMS possesses several physical qualities, including as its remarkable elasto-optic and thermo-optic capabilities, high optical transparency, low absorption across a wide range of wavelengths, and biocompatibility [7]. Polydimethylsiloxane can be employed in various temperature-sensing applications due to its affordability, uncomplicated production method, and high thermo-optic coefficient. This includes scenarios that require a high level of sensitivity [3]. This polymer exhibits a distinctive amalgamation of characteristics due to the presence of both an inorganic siloxane backbone and organic methyl groups bonded to silicon. A low glass transition temperature renders the substance in a fluid state at ambient temperature. The fluid substance can be rapidly and easily transformed into a solid elastomer by the process of cross-linking. PDMS-based devices exhibit significant sensitivity to temperature variations due to their elevated thermo-optic coefficient [4]. This work reports a numerical investigation of a temperature sensor designed using 3D PhC structures based on low-index dielectric materials, i.e, niobium pentoxide (Nb<sub>2</sub>O<sub>5</sub>) and silicon dioxide (SiO<sub>2</sub>). The sensor operates based on the principle of refractive index sensing using Fano-resonance in the near-infrared wavelength region. A PDMS functional layer is applied on top of the waveguide layer, and its physical properties undergo changes in response to temperature fluctuations. The change in temperature causes a variation in the refractive index of the PDMS layer, which in turn is detected by a shift in the resonant wavelength  $\lambda_{res}$ . The sensor device's performance is assessed based on the shift in  $\lambda_{res}$ , alteration in the linewidth of the resonant modes, sensitivity (S), and figure-of-merit (FOM). The device has excellent performance and utilizes a straightforward light-coupling approach. This positions it as a formidable competitor to several complicated sensing devices, like MIM-waveguide-based temperature sensors.

### Materials and Methods

The finite-difference time-domain (FDTD) method was utilized for numerical modeling and simulation. This was carried out in MEEP, an open-source software platform developed at MIT University specifically for electromagnetic equation propagation. MEEP-FDTD utilizes Maxwell's equations to compute the propagation of the electromagnetic (EM) field within the medium. A Gaussian pulse source is employed to compute the system's response across a broad spectrum of frequencies in a single execution. The simulation is initialized with a center wavelength of the source,  $\lambda_c$ , set to

1.46 nm, and a pulse width,  $df$ , of 0.15 in terms of frequency. The flux is calculated at numerous frequency points,  $nf$ , with a total of 6000 points. The simulation domain was established with a resolution of 30, which was sufficient to capture the smallest structural feature and calculate the lowest wavelength component. Figure 1a displays a 3D representation of the sensor design. In this design, the waveguide layer is placed on top of the SiO<sub>2</sub> substrate, and air-hole-based photonic crystal (PhC) elements are arranged across the waveguide layer.

The SiO<sub>2</sub> substrate has a refractive index of 1.5, whereas the Nb<sub>2</sub>O<sub>5</sub> waveguide has a refractive index of 2.2 in the 1500 nm spectral range. The refractive index values are obtained as a point of reference from sources [2,4]. The lattice constant of the structure (Figure 1a) is set to a value of 1000 nm in order to facilitate the operation of the device within the near-infrared spectral range. Figure 1b illustrates a simplistic unit cell simulation model employed in this study. The simulation cell is bounded by perfectly matched layer (PML) boundary conditions in the top and

lower Z-directions. The PML layer has a predetermined thickness of  $\lambda$  nm in order to fully absorb the entire electromagnetic spectrum produced by the source at the borders. Furthermore, the unit cell model is replicated in the horizontal (X and Y) directions by employing periodic boundary conditions (PBC) offered by the simulation software. The plane wave excitation source is positioned directly above the structure (Figure 1b), whereas the transmission and reflection flux of the resonant modes are estimated below and above the waveguide, respectively. The software allows the user to provide a custom-configured monitoring point for field decay, which will end the simulation when the required field decay condition is met. A field decay monitor point is positioned beneath the transmission monitor layer, as depicted in Figure 1b. The software automatically converts the simulation results from the time domain to the frequency domain using a Fourier transform in order to facilitate their viewing.

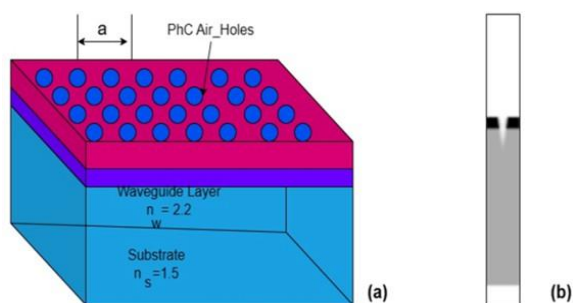


Figure 1: Simulation model of proposed thermal sensor (a) A 3D model of the sensor device with an indication of substrate, waveguide, air hole, and lattice constant (b) Unit cell simulation model of PhC Structure in HD5 file

### Sensing mechanism

The design parameters of the PhC structure were initially optimized to achieve an effective wavelength filtering mechanism, resulting in the emergence of a narrowband Fano resonance at  $\lambda_{res} = 1470$  nm. The waveguide's thickness was set to 330 nm based on optimum design parameters. A layer of PDMS was applied onto the waveguide layer, allowing the PDMS material to infiltrate and occupy the air holes. The PDMS layer served as a functional layer, exhibiting varying physical qualities in response to changes in the surrounding temperature. In order to optimize the process, certain parameters are simulated, such as the radius values of 0.20, 0.24, and 0.28, the PDMS values of 0.27, 0.33, and 0.45, and the hole depth (h) values of 1.0 and 1.5. The best results are obtained at the PDMS value of 0.33, radius at 0.20. Figure 2b provides a cross-sectional view of the unit cell model, illustrating the PDMS functional layer, PDMS-filled PhC hole, and the surrounding atmosphere where the temperature change was observed.

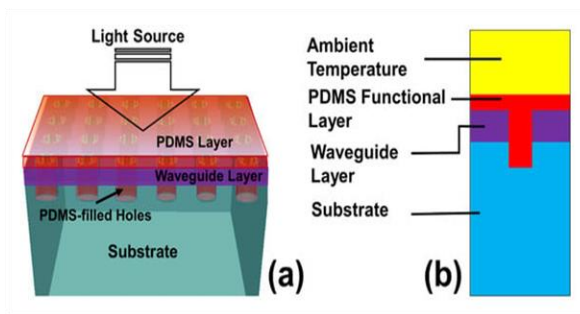


Figure 2. Thermal sensing mechanism of the device: (a) A PDMS functional layer was deposited on the top and filled in the PhC holes. Light source incident on the device to excite the Fano-resonances; (b) Unit cell model with PDMS functional layer and ambient atmosphere where the temperature change was to be measured.

The relationship between the refractive index of the PDMS material and temperature  $T$  (in  $^{\circ}\text{C}$ ) was obtained from previous studies [7–9]. This relationship is described by Equation (1). Figure 3 illustrates the visual representation of the aforementioned relationship. It is evident that the refractive index of PDMS exhibits a linear variation from 1.4131 to 1.3741 as the temperature ranges from 0 to 110  $^{\circ}\text{C}$ . The developed sensor device was numerically examined for its design and performance as an optical thermal sensor, utilizing this correlation.

$$n_p(T) = 1.4176 - 4.5 \times 10^{-4} \cdot T$$

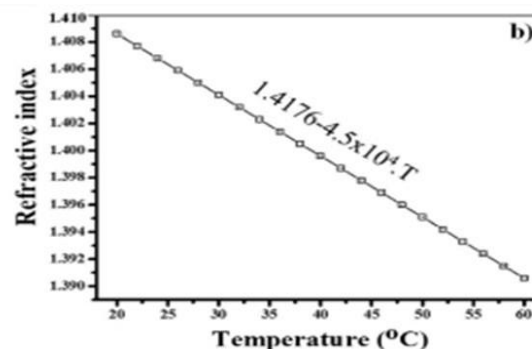


Figure 3. Refractive index variation of PDMS as a function of ambient temperature

### Design Parameters Optimization

In order to maximize the sensitivity of the proposed model, the structural design parameters were adjusted throughout a range of values. The design parameters are subject to variation. The spectral features were measured at three important plan boundaries: the thickness of the PDMS layer, the depth of the PhC holes, and their radius. The figures clearly indicate that the linewidth has successfully achieved its fundamental characteristics. The optimal values for the plan parameters to test the device as a thermal sensor were selected as  $w = 0.33$ ,  $h = 1.5$ , and  $r = 0.20$ . It is calculated by the equation  $y = a + b \cdot x$ .

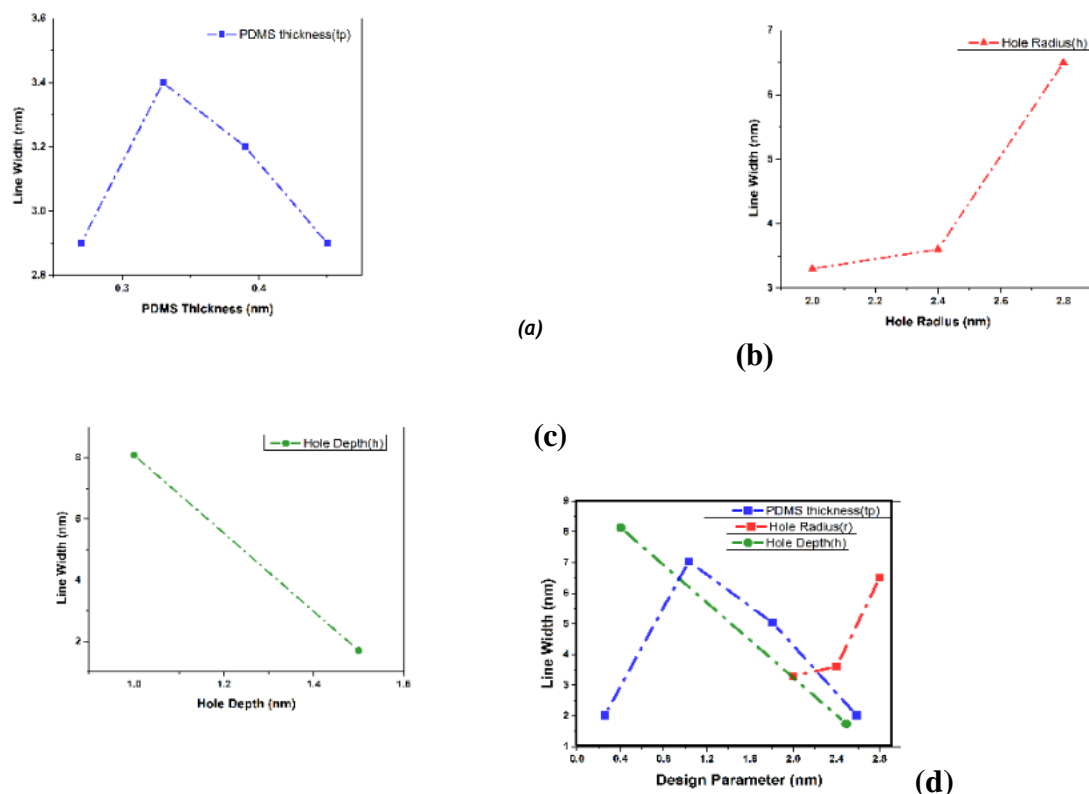


Figure 4. (a) PDMS thickness vs. Line width; (b) Hole Radius vs. Linewidth; (c) hole Depth vs. Linewidth; (d) : Design parameters vs. Linewidth

#### Temperature sensor at 0 to 110°:

The graph illustrates the temperature fluctuations ranging from 0 to 110. The optimal values are assessed to be 0.33(tp) PDMS with a radius (r) of 0.20, a hole depth (h) of 1.5, and a radius (r) of 0.20. The temperature has a direct impact on the refractive error of the PDMS layer, causing a change of 0.33 nm. The sensor generates a distinct resonance. The transmission spectra were observable across a temperature range of 0 to 110 degrees Celsius. The temperature transition from 0 to 110 is illustrated in the accompanying figure, along with the graph representing the aforementioned relationship. The refractive index of PDMS exhibited a consistent and proportional decrease, transitioning from 1.4131 to 1.3741.

The design parameters of the PhC structure were modified in order to enhance its wavelength filtering mechanism. The temperature-sensing resonant wavelength was adjusted to 1490 nm while keeping the waveguide thickness constant at 0.33 nm. The device exhibited excellent performance in terms of sensitivity (S), variations in resonance frequency line width, and figure of merit (FOM). The calculations indicate that the sensor's resonant wavelength falls between the range of 15302.05 to 1507.23 nm. The linewidth of the sensor is 2.0 rad, and its sensitivity ranges from 0.1114302 to 0.13124344. Additionally, the figure of merit (FOM) for the sensor is between

0.032774 and 0.03235.

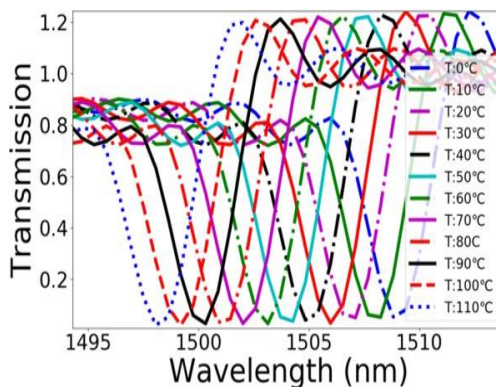


Figure 6: Temperature variation from 0 to 110

#### Proposed Method for the Preparation of Thermal Sensor:

The process of precisely developing a structure is quite intricate and requires a significant amount of time. Obtaining the exact values of a structure's parameter necessitates addressing a multitude of circumstances. The first step involves the deposition of PDMS polymer onto the holes of the photonic crystals using a simple single cell model, despite the fact that the polymer is both flexible and in a liquid state. After filling the hole, a new layer, known as the function layer, is formed on the surface of the photonic crystal. We employed a temperature-variant setting on polymers for the purpose of biosensing experimentation. This resulted in a variation in the refractive index of the polymers based on the temperature. Low temperature corresponds to a high reflecting index, while high temperature corresponds to a low reflective index. Below is a detailed guide outlining the step-by-step preparations.

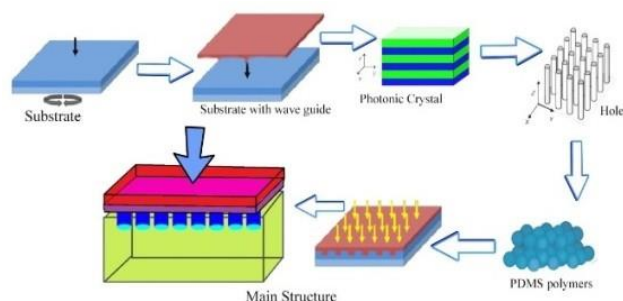


Fig 6: Steps of designing thermal sensor.

#### Comparative analysis:

Various thermal sensors have been described in the literature, such as periodic structures like photonic crystals or nanogratings, plasmonic structures, fiber-optic-based sensors,

interferometer-based designs, and thermal sensors that utilize fiber-optic technology. Plasmonic sensors often offer enhanced sensitivity, while their production is challenging and costly. Dielectrics and polymers have been widely publicized as potential materials for thermal sensors. Fiber-optic sensors possess the advantage of a pre-existing waveguide, and additional configurations can be integrated into them for detection purposes. PDMS has been employed in several sensing applications, including as refractive index detection, gas detection, and thermal detection. An analogous analysis of this piece is presented in a Table that illustrates the contrast between the planned work and the existing literature.

Table 1. Comparison of the proposed work with the existing literature

Measurement Range(°C)	Sensitivity(nm/° C)	Researched work
20 to 85	0.075	9
20 to 100	0.101	10
20 to 100	0.22	11
20 to 30	-1.63	12
0-90	0.109	[1]
0-110	0.1114302	Thesis work

### Conclusion:

The mathematical analysis of a temperature sensor device based on Dielectric PhCs, operating at a wavelength of 1470 nm in the telecommunication spectral region, has been conducted. This gadget is affordable, user-friendly, and operates within the 1470 nm wavelength range. An all-solid stacking waveguide was constructed on a SiO<sub>2</sub> substrate that contains air-hole based PhC holes. Niobium pentoxide is the subsequent layer following the wave guide layer. The most favorable design parameters were determined to be  $t_p = 0.33$  nm for the PDMS layer,  $h = 1.5$  nm for the depth of the PhCholes, and  $r = 0.20$  nm for the hole radius. The suggested device operates at a wavelength of 1470 nm and has a typical linewidth of 3.4 nm. The voids in the photonic crystal were filled, and a layer of PDMS was applied on top of the waveguide layer with a thickness of  $t_p = 0.33$  nm for the purpose of temperature sensing. With an increase in temperature, the refractive index of PDMS decreased. Analyzed analytically, the sensor response was examined in a thermal range of 0 to 110 C, with the refractive index varying from 1.4131 to 1.3741. The maximum values for S and FOM were defined as 0.1114302 and 0.032774 nm/C, respectively. The sensor's performance and presentation, also known as the figure of merit (FOM), can be evaluated based on its sensitivity (S), resolution (Res), and line width (Lw). Additionally, a figure of merit (F) is used to assess the sensor's overall performance. The light connection technique is uncomplicated, and the sensor exhibits excellent performance. Therefore, it poses a significant challenge to more sophisticated systems available in the market, such as MIM-wave guide temperature sensors. Considering the characteristics of the active compound, the capacity to withstand heat, and the cost-effectiveness of the dielectric materials used, the sensor device can be suggested for a wide

range of temperature detection applications by using a straightforward arrangement of optical fibers.

This study examines the development of an optical thermal sensor using polydimethylsiloxane polymers, utilizing the widely-used MEEP python simulation approach. Its purpose is to generate replicated outcomes for 3D photonic crystal formations.

**Institutional Review Board Statement:** Not applicable. **Informed Consent Statement:** Not applicable.

Data Availability Statement: Not applicable.

**Acknowledgments:** The authors are grateful to the Nanophotonics Research Group at BUITEMS Quetta for their contribution to making this research work possible.

**Conflicts of Interest:** The authors declare no conflict of interest.

## References

- Khan, Y.; Butt, M.A.; Khonina, S.N.; Kazanskiy, N.L. Thermal Sensor Based on Polydimethylsiloxane Polymer Deposited on Low-Index-Contrast Dielectric Photonic Crystal Structure. *Photonics* 2022, 9, 770. <https://doi.org/10.3390/photonics9100770>
- Ma L, Zhang Y, Zhang W, Li Z, Gao H, Ma H, et al. High-performance all-fiber Mach-Zehnder interferometer based on D-shaped two-mode fiber coated with polydimethylsiloxane for temperature sensing. *Optical Fiber Technology*. 2022; 71:102924.
- Amiri IS, Azzuhri SRB, Jalil MA, Hairi HM, Ali J, Bunruangses M, et al. Introduction to photonics: Principles and the most recent applications of microstructures. *Micromachines*. 2018;9(9):452.
- Arianejad MM, Amiri IS, Ahmad H, Yupapin P. A large free spectral range of 74.92 GHz in comb peaks generated by SU-8 polymer micro-ring resonators: simulation and experiment. *Laser Physics*. 2018;28(11):115002.
- Batumalay M, Johari MAM, Khudus MIMA, Jali MHB, Al Noman A, Harun SW, editors. Microbottle resonator for temperature sensing. *Journal of Physics: Conference Series*; 2019: IOP Publishing.
- Zeng X, Wu Y, Hou C, Bai J, Yang G. A temperature sensor based on optical microfiber knot resonator. *Optics Communications*. 2009;282(18):3817-9.
- Aly AH, Mohamed D, Mohaseb MA, Abd El-Gawaad N, Trabelsi Y. Biophotonic sensor for the detection of creatinine concentration in blood serum based on 1D photonic crystal. *RSC advances*. 2020;10(53):31765-72.
- Taflove A. Application of the finite-difference time-domain method to sinusoidal steady-state electromagnetic-penetration problems. *IEEE Transactions on electromagnetic compatibility*. 1980(3):191-202.
- Yang, W., Li, C., Wang, M., Yu, X., Fan, J., Xiong, Y., ... & Li, L. (2020). The polydimethylsiloxane coated fiber optic for all fiber temperature sensing based on the multithin–multifiber structure. *IEEE Sensors Journal*, 21(1), 51-56.
- Gong, J., Shen, C., Xiao, Y., Liu, S., Zhang, C., Ding, Z., ... & Chen, Y. (2019). High sensitivity fiber temperature sensor based PDMS film on Mach-Zehnder interferometer. *Optical Fiber Technology*, 53, 102029.
- Wang, F., Lu, Y., Wang, X., Ma, T., Li, L., Yu, K., ... & Chen, Y. (2021). A highly sensitive temperature sensor with a PDMS-coated tapered dispersion compensation fiber structure.

- Optics Communications, 497, 127183.
- Wang, H.; Liao, M.; Xiao, H.; Han, X.; Jiang, Y.; Tan, J.; Zhang, P.; Shao, J.; Tian, Y.; Yang, J. High sensitivity temperature sensor based on a PDMS-assisted bow-shaped fiber structure. *Opt. Commun.* 2021, 481, 126536.
- Toppr. Propagation of Electromagnetic Waves
- Torino S, Conte L, Iodice M, Coppola G, Prien RD. PDMS membranes as sensing element in optical sensors for gas detection in water. *Sensing and bio-sensing research.* 2017; 16:74-8.
- Uno T, He Y, Adachi S. Perfectly matched layer absorbing boundary condition for dispersive medium. *IEEE Microwave and Guided wave letters.* 1997;7(9):264-6.
- van Leest T, Caro J. Cavity-enhanced optical trapping of bacteria using a silicon photonic crystal. *Lab on a Chip.* 2013;13(22):4358-65.
- Wang H, Liao M, Xiao H, Han X, Jiang Y, Tan J, et al. High sensitivity temperature sensor based on a PDMS-assisted bow-shaped fiber structure. *Optics Communications.* 2021; 481:126536.
- Wang P, Ding M, Bo L, Guan C, Semenova Y, Wu Q, et al. Fiber-tip high-temperature sensor based on multimode interference. *Optics letters.* 2013;38(22):4617-20.
- Wang S, Magnusson R. Theory, and applications of guided-mode resonance filters. *Applied optics.* 1993;32(14):2606-13.
- Wang S. Finite-difference time-domain approach to underwater acoustic scattering problems. *The Journal of the Acoustical Society of America.* 1996;99(4):1924-31.
- Lourtioz J-M, Benisty H, Berger V, Gerard J-M, Maystre D, Tchelnokov A. Photonic crystals. *Towards Nanoscale Photonic Devices.* 2005.
- Lukacova-Medvid ova M, Warnecke G, Zahaykah Y. On the boundary conditions for EG-methods applied to the two-dimensional wave equation system. *ZEITSCHRIFT FUR ANGEWANDTE MATHEMATIK UND MECHANIK.* 2004;84(4):237-51.
- Magnusson R, Shokooch-Saremi M, Lee KJ, Curzan J, Wawro D, Zimmerman S, et al., editors. Leaky-mode resonance photonics: an applications platform. *Nanoengineering: Fabrication, Properties, Optics, and Devices VIII;* 2011: SPIE.
- Marsh R, Shapiro M, Temkin R, editors. Photonic bandgap (PBG) accelerator structure design. *2007 IEEE Particle Accelerator Conference (PAC);* 2007: IEEE.
- Monzon JC. On surface integral representations: validity of Huygens' principle and the equivalence principle in inhomogeneous bianisotropic media. *IEEE transactions on microwave theory and techniques.* 1993;41(11):1995-2001.
- Moraleda AT, García CV, Zaballa JZ, Arrue J. A temperature sensor based on a polymer optical fiber macro-bend. *Sensors.* 2013;13(10):13076-89.
- Mur G. Absorbing boundary conditions for the finite-difference approximation of the time-domain electromagnetic-field equations. *IEEE transactions on Electromagnetic Compatibility.* 1981(4):377-82.
- Murtaza G, Rizvi AS, Irfan M, Yan D, Khan RU, Rafique B, et al. Glycated albumin based photonic crystal sensors for detection of lipopolysaccharides and discrimination of Gram-negative bacteria. *Analytica chimica acta.* 2020; 1117:1-8.
- Nair RV, Vijaya R. Photonic crystal sensors: An overview. *Progress in Quantum Electronics.* 2010;34(3):89-134.

Nico C, Soares M, Rodrigues J, Matos M, Monteiro R, Graça M, et al. Sintered NbO powders for electronic device applications. *The Journal of Physical Chemistry C*. 2011;115(11):4879-86